EDGE ARTICLE

Check for updates

Single-molecule photoredox catalysis†

Josef Haimerl,[a] Indrajit Ghosh,[b] Burkhard König, [iD][b] Jan Vogelsang[a] and John M. Lupton [iD] *[a]

The chemistry of life is founded on light, so is it appropriate to think of light as a chemical substance? Planck's quantization offers a metric analogous to Avogadro's number to relate the number of particles to an effective reaction of single molecules and photons to form a new compound. A rhodamine dye molecule serves as a dehalogenating photocatalyst in a consecutive photoelectron transfer (conPET) process which adds the energy of two photons, with the first photon inducing radical formation and the second photon triggering PET to the substrate molecule. Rather than probing catalytic heterogeneity and dynamics on the single-molecule level, single-photon synthesis is demonstrated: the light quantum constitutes a reactant for the single substrate molecule in a dye−driven reaction. The approach illustrates that molecular diffusion and excited-state internal conversion are not limiting factors in conPET reaction kinetics because of catalyst−substrate preassociation. The effect could be common to photoredox catalysis, removing the conventional requirement of long excited-state lifetimes.

Introduction

Photosynthesis is the archetypal photocatalytic process. Having evolved from primordial life over billions of years, the conversion of sunlight into chemical energy remains enigmatic at once in its elegance and complexity. Whereas nature combines the energy of multiple photons to drive the conversion of carbon dioxide and water into carbohydrates, even the simplest artificial models of consecutive photoelectron transfer (conPET) synthesis have proven challenging to realize in the laboratory.[1–7] Most photocatalysts involve expensive heavy-metal elements, but recently, the potential of hydrocarbon dyes in organic photocatalysis has emerged.[8–11] First reports have shown that even common organic dyestuffs such as perylene[12] or rhodamine[13–15] function as effective organic photocatalysts. Since one of the goals of photocatalysis is to achieve cheap large-scale conversion of materials, single-molecule techniques have received only limited attention as an avenue to exploring and optimizing catalytic efficiency.[16] But since, ultimately, photocatalysis is a molecular process, only microscopic spectroscopic techniques can provide truly mechanistic insights for quantum-chemical models.[17–19] The main focus to date of the technique in the context of photocatalysis has been on exploring the spatial and temporal heterogeneity of reactions[20–25] involving either single-photon mediated processes,[26] or using chemical conversion of a dye molecule to track catalytic activity.[27–30] In addition, single-molecule techniques have proven versatile in imaging protein-based reactions,[31–35] and single-electron transfer events in general.[36,52] Little attention has been paid to actually driving chemical reactions on the single-molecule level, with most prior interest directed at the potential of scanning-probe techniques in electrically catalysed reactions for lithographic applications.[37–41]

Few experiments illustrate the particle nature of light more directly than single-photon counting. Passing the fluorescence of a single molecule through a semi-transparent mirror, a beam splitter, with single-photon detectors on either side will give rise to a pronounced anticorrelation in time between the two detectors: photon antibunching occurs, since the same photon cannot be picked up by both detectors.[42] This antibunching arises on timescales of the excited-state lifetime of the molecule, *i.e.* typically several nanoseconds. On longer timescales, the opposite effect occurs: the fluorescent molecule undergoes quantum jumps between bright and dark states, for example between the singlet and the triplet manifolds of the excited state, leading to bunching of photons in time.[43] This cycling between emissive and non-emissive states of the fluorophore provides crucial insight into the molecular quantum jumps responsible for the photosynthetic reaction.[44]

Here, we exploit the versatile method of single-molecule spectroscopy to probe the conPET process, one photon at a time. Fig. 1a illustrates a prototypical model process of aqueous organic photocatalysis exploiting consecutive photoelectron transfer (conPET).[13] Absorption of a photon of energy $h\nu_1$ by a rhodamine-6G (Rh6G) dye molecule leads to the formation of an excited singlet state. This singlet can undergo either radiative relaxation to the ground state by fluorescing, convert into a triplet by intersystem crossing, or interchange

[a]*Institut für Experimentelle und Angewandte Physik, Universität Regensburg, 93040 Regensburg, Germany. E-mail: john.lupton@ur.de*

[b]*Institut für Organische Chemie, Universität Regensburg, 93040 Regensburg, Germany*

† Electronic supplementary information (ESI) available. See DOI: 10.1039/c8sc03860k

Fig. 1 A model dye-based photocatalytic reaction enabling addition of photon energy by consecutive photoelectron transfer (conPET). (a) A cationic rhodamine 6G (Rh6G) dye molecule in phosphate-buffered saline (PBS) is excited by a photon of energy $h\nu_1$ and is subsequently reduced by ascorbic acid (AscA) to form a radical. A second photon $h\nu_2$ excites the radical, leading to PET to the halogenated substrate 2-bromobenzonitrile (BrBN). Note that since in the single-molecule experiments it is the dye and not the product yield which is monitored, a trapping agent is not needed for this reaction. (b) Synthetic-scale C–H aromatic substitution of 2-bromobenzonitrile with an N-methylpyrrole trapping agent in an aqueous mixture of dye, substrate, reducing and trapping agent under two-colour LED illumination in the green ($h\nu_1$) and blue ($h\nu_2$). The conversion yield after 24 hours as determined by gas chromatography is 94%. Note that synthetic-scale reactions are usually carried out with LEDs rather than lasers. Lasers are necessary to focus light tightly in single-molecule experiments. Since the absorption spectrum of the radical state is broad, the reaction works for both blue wavelengths ($h\nu_2$) of 405 nm (laser) and 455 nm (LED).

charge with reductants to form a radical. If the latter two processes occur, the dye molecule will cease to fluoresce for a short period of time, on the order of a few microseconds up to milliseconds.[52] Addition of a reducing agent, ascorbic acid, promotes formation of the rhodamine radical from either the singlet or the triplet state. Since Rh6G in water is cationic,[45] electron transfer from the reducing agent will form the neutral Rh6G radical R·. This radical is characterised by a certain lifetime, and will ultimately relax to the cationic ground state by

shedding the additional electron to the environment. The reduction potential of the R· ground state of −1 V vs. SCE[13] is too low for electron transfer to occur to a substrate molecule to cleave stable bonds in aryl halides, such as in the dehalogenation of 2-bromobenzonitrile. Such a reaction requires a reduction potential of −1.9 V vs. SCE.[13,46,47] The additional energy necessary to achieve this is made available by re-exciting the radical with a second photon of energy $h\nu_2$. The reduction potential of the excited radical state of Rh6G, R·*, is −2.4 V vs. SCE,[13] which is sufficient for dehalogenation of the substrate. The second photon, in combination with the electron transfer to the substrate, therefore removes the additional electron from the dye radical, returning the dye to the ground state and thereby reactivating the $S_1 \rightarrow S_0$ fluorescence cycle. The water-based mechanism proposed here is, in principle, analogous to reaction cycles recently described in organic solvents.[13] Fig. 1b states the synthetic-scale C–H aromatic substitution reaction of 2-bromobenzonitrile in water, using a reaction mixture containing the dye, substrate, and reducing agent, along with an additional trapping agent, N-methylpyrrole. The reaction occurs under continuous illumination with two light-emitting diodes (LEDs). The conversion yield after 24 hours determined by gas chromatography (GC) is 94%. Chromatograms of the product of this reaction and several control reactions are shown in Fig. S1 of the ESI.† This simple cycle constitutes one of the first reports of a C–H arylation by an organic dye in water and is therefore likely to be of interest in a range of aqueous biochemical reactions.[13] Note that the additional trapping agent is only required in the ensemble reaction, where the product yield is monitored, and not in the single-molecule experiments, where the dye acts as the reporter on the reaction. Since the absorption spectrum of the radical is broad, the conPET cycle appears to work with a range of different photon energies. For experimental reasons, different light sources and wavelengths are used for the single-molecule and synthetic-scale reactions.

Even though this conPET cycle apparently works, it is not at all clear how a conventional dye molecule actually enables consecutive photoredox catalysis. Internal conversion is the most efficient process of energy dissipation from higher-lying states in molecules, and a photoexcited radical is expected to shed excess energy to the environment within a few hundred femtoseconds, as documented by transient absorption spectroscopy.[48] Such ultrafast energy dissipation inhibits intermolecular photoreactions and would certainly prevent any diffusion-driven process from occurring in solution.

Results and discussion

Single-molecule imaging

In order to study the conPET mechanism on the single-molecule single-photon level, the photocatalytically active dye molecules have to be immobilized on a surface to prevent diffusion in the solvent.[49] We therefore tether the dyes to DNA oligomers, functionalised with biotin–streptavidin linkers, as sketched in Fig. 2a. These linkers bind to biotinylated bovine serum albumin (BSA) covered glass substrates at sufficiently low concentration so that they can be resolved individually in
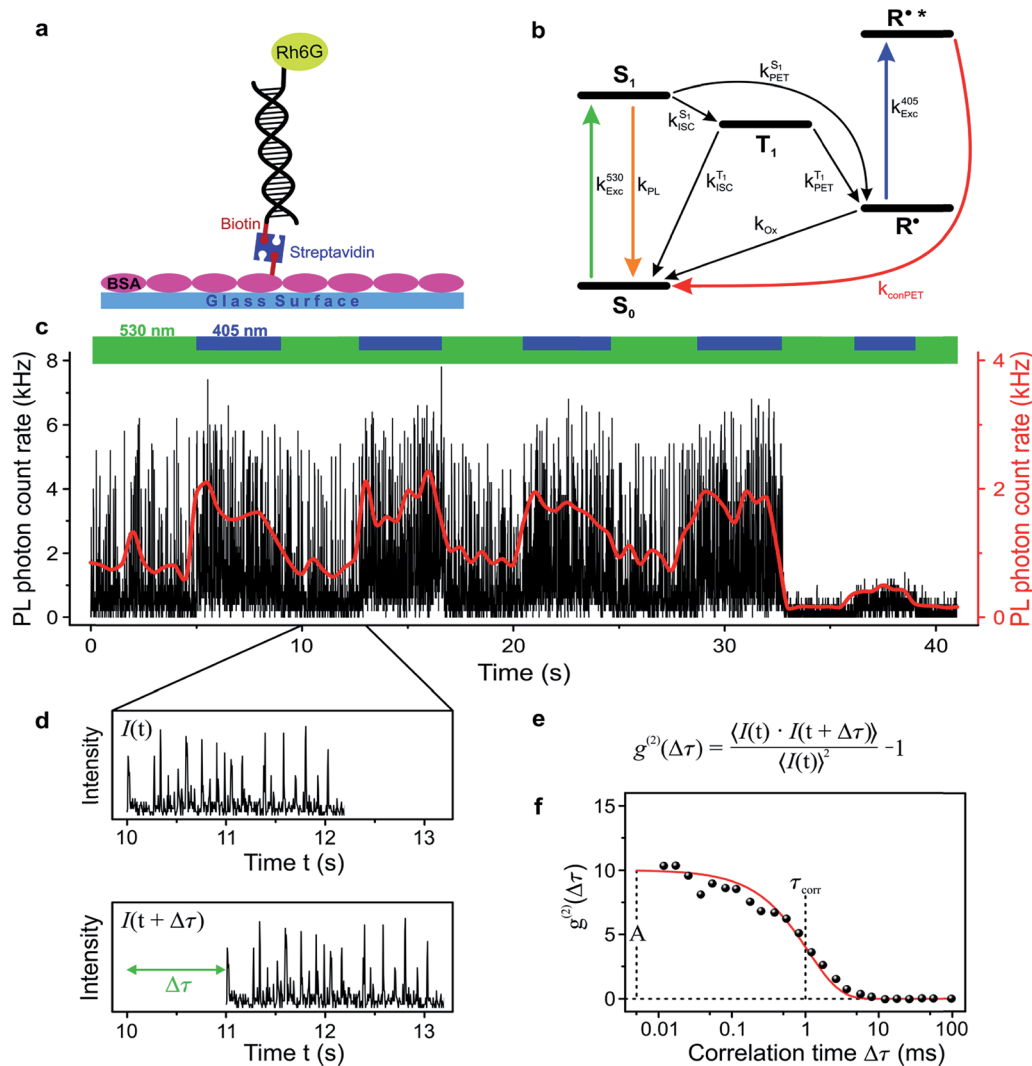
Fig. 2 Single-molecule imaging of the conPET cycle. (a) To track the reaction on the single-molecule level, the dye is immobilized by tethering to a glass substrate with functionalized DNA strands. (b) Energy-level scheme describing the possible excited-state transitions of the rhodamine dye. (c) Example fluorescence trace of a single dye molecule under constant illumination with $h\nu_1$ and alternating illumination with $h\nu_2$. The fluorescence appears as intensity spikes. The spike intensity is not increased by $h\nu_2$, implying that there is no additional photocycling of the dye molecule by the superimposed illumination. In contrast, the frequency of the spikes increases under irradiation with $h\nu_2$, implying that the dark-state lifetime is reduced. (d) Close-up of the fluorescence trace, showing distinct periods of fluorescence over a duration of τ_{on} separated by dark periods of duration τ_{off}. (e) Information on fluctuations of the fluorescence is extracted by cross-correlating the fluorescence intensity, *i.e.* by computing the time average of the product of the fluctuation signal with itself, shifted by a delay time $\Delta\tau$. The equation states the correlation amplitude $g^{(2)}$ as a function of delay time $\Delta\tau$. (f) Plot of a typical fluorescence correlation signal with a single-exponential fit of amplitude A and correlation lifetime τ_{corr}, allowing the exctraction of characteristic "on" and "off" times in the single-molecule fluorescence.

a confocal fluorescence microscope. Fig. 2b indicates the anticipated level scheme of the Rh6G dye molecules. Fluorescence is observed from the single molecules as long as they cycle between S_0 and S_1 states. Excursions to the triplet or the radical state lead to a disruption of this cycle and inhibit fluorescence. The triplet can relax back to the ground state by reverse inter-system crossing with a rate of $k_{ISC}^{T_1}$, or else be reduced to form the radical of the dye molecule. In the presence of a reducing agent, the singlet can also be reduced to form the radical, which can re-oxidise at an intrinsic rate, returning the dye molecule to its ground state; or else the radical can be photoexcited again to form R⁺*, which can transfer its electron to the substrate molecule 2-bromobenzonitrile.

To test the feasibility of tracking the conPET cycle on the single-molecule level, we plot the fluorescence of a single teth-ered Rh6G molecule in Fig. 2c as a function of time, binned in intervals of 5 ms, with alternating application of $h\nu_2$. The fluo-rescence intensity, stated in terms of the photon count rate, appears as bursts of approximately equal strength, separated by prolonged intervals of darkness. The average photon count rate, binned over intervals of 0.5 s, is superimposed in the plot as a red line. As the dye radical is re-excited by $h\nu_2$, the number of fluorescence spikes increases and the average brightness of the single molecule (red line) doubles. The height of the individual spikes remains almost constant, implying that it is not the number of photons absorbed by the dye which increases upon

simultaneous excitation at two wavelengths. Rather, the intermittency between bursts is shortened. Panel d plots a two-second interval of the fluorescence trace of panel c, revealing distinct "on" and "off" periods of the molecular fluorescence. Such intermittency can be used to analyse the fluorescence to extract characteristic timescales τ_{on} and τ_{off}. Fitting directly to fluorescence intermittency traces is cumbersome and limited in time resolution by the finite photon count rate. A versatile quantification of the fluorescence dynamics is instead offered by a single-photon correlation analysis of the fluorescence intensity.[50] As indicated in panel e, the correlation is computed by calculating the self-convolution, *i.e.* the time average of the product of the trace with itself, shifted by a temporal offset of $\Delta\tau$. Fig. 2f shows the result of such a typical cross-correlation, plotted on a logarithmic time axis. The correlation can be fitted with a single-exponential function of the form $g^{(2)}(\Delta\tau) = A \times \exp\left(-\dfrac{\Delta\tau}{\tau_{corr}}\right)$, where A is the correlation amplitude, τ_{corr} is the characteristic decay time of the correlation, and the "on" and "off" times of the molecular fluorescence are related by $\tau_{on} = \tau_{corr}(1 + 1/A)$ and $\tau_{off} = \tau_{corr}(1 + A)$.[50] By adding up τ_{on} and τ_{off}, we determine the single-molecule turnover frequency $TOF_{SM} = 1/(\tau_{on} + \tau_{off})$. This number of cycles which one single dye molecule undergoes through the dark state sets the upper limit for synthetic-scale TOF. Details of the fluorescence microscopy, including the background correction procedure, are summarized in the ESI.†

Single-molecule photon-correlation spectroscopy

We analyse the photocatalytic cycle using fluorescence intensity correlation spectroscopy. We stress that this analysis is only possible on the single-molecule level, since in the ensemble the molecular excursions to the dark state and the associated fluctuations in fluorescence intensity are averaged out. Each single-molecule fluorescence-intensity trace gives an individual photon correlation curve. To account for the statistical variation between different single molecules, we consider the median value of one hundred single-molecule correlation curves for each value of $\Delta\tau$, plotted with exponential fits in Fig. 3. We begin in panel a by examining the fluorescence correlation in nitrogen-saturated phosphate-buffered saline (PBS) for the case of excitation with photon energy $h\nu_1$. Under these conditions, the regular transitions of the dye molecule to the triplet manifold give rise to a well-defined "off" time, which can be attributed to the triplet-state lifetime or the lifetime of a radical formed out of the triplet. The temporal excursions to such a dark state are indicated in the cartoon to the right, with $\tau_{on} = 2.22 \pm 0.02$ ms, $\tau_{off} = 5.99 \pm 0.09$ ms, and $TOF_{SM} = 123$ s^{-1}. The Rh6G triplet state is quenched by molecular oxygen, by saturating the solvent with air. When this quenching occurs, the dye molecule cycles solely between ground and excited singlet state: no amplitude exists in the photon correlation signal in panel b, implying the absence of a dark state.

To monitor the molecular dynamics relating to PET, we carry out the following experiments under conditions where the dark state is stabilised, *i.e.* under nitrogen saturation. Panel c plots the photon correlation with addition of the reducing agent

ascorbic acid. Now, the molecular dark state must be attributed to the radical with $\tau_{on} = 1.73 \pm 0.03$ ms, $\tau_{off} = 21.3 \pm 0.5$ ms, and $TOF_{SM} = 44$ s^{-1}. Adding the substrate compound 2-bromobenzonitrile in panel d has no effect on the correlation and the associated timescales. In contrast, exciting the radical with $h\nu_2$ in the absence of the substrate in panel e promotes depopulation of the radical state, shortening the dark-state lifetime to $\tau_{off} = 8.4 \pm 0.3$ ms, with $\tau_{on} = 1.5 \pm 0.05$ ms, and $TOF_{SM} = 100$ s^{-1}.[53] The dramatic effect arises upon simultaneous addition of the two reactants – $h\nu_2$ photons and 2-bromobenzonitrile molecules – to the dye catalyst. The correlation amplitude in panel f is suppressed almost entirely, but characteristic "on" and "off" times can still be determined as $\tau_{on} = 2.6 \pm 0.2$ ms, $\tau_{off} = 4.7 \pm 0.4$ ms, and $TOF_{SM} = 137$ s^{-1}. The additional 37 photocycles per second undergone by the catalyst in the presence of the substrate provide a metric for the overall upper limit of the dehalogenation reaction efficiency. Under these reaction conditions, each single Rh6G molecule dehalogenates 37 2-bromobenzonitrile molecules per second.

In order to prove chemical specificity of the microscopic photocatalytic conPET cycle, it is necessary to demonstrate that the dark state of the dye is not quenched for substrate molecules which cannot be dehalogenated. The obvious material to test this is the non-halogenated compound benzonitrile. Fig. 4a plots the single-molecule correlation signal for the four conditions used in Fig. 3c–f, but with benzonitrile added as the substrate. As before, the correlation is identical with only the reducing agent ascorbic acid added (black curve) and with ascorbic acid and benzonitrile combined (red curve) in the solution. Excitation of the Rh6G radical with $h\nu_2$ shortens the dark-state lifetime by returning the dye from the radical state to the ground state (light–blue curve). However, in contrast to the situation in Fig. 3, addition of benzonitrile has no effect on the photon correlation trace (dark–blue curve). We conclude that benzonitrile does not interact with the photocatalyst since addition of it to the solution has no effect on the fluorescence cross-correlation. This conclusion is crucial since otherwise product inhibition of the catalyst would occur by the dehalogenated substrate, disrupting the photon cycling process. Once bromine is cleaved from 2-bromobenzonitrile, the molecule disassociates from the catalyst of Fig. 1. An alternative test of the reaction is performed with 4-chloroanisole, as summarized in Fig. 4b. This substrate is energetically not expected to undergo bond cleavage by the excited radical R$^{•}$*, as the reduction potential necessary amounts to -2.9 V *vs.* SCE.[45] Indeed, in Fig. 4b no effect is seen on the correlation curves of addition of the 4-chloroanisole substrate at the same concentration as that used in Fig. 3.

Discussion

The single-molecule conPET cycle demonstrated here effectively constitutes a single-photon chemical reaction: the first photon $h\nu_1$, in combination with a reducing agent, generates the photocatalyst – the rhodamine radical – which subsequently reacts the two "compounds", the substrate 2-bromobenzonitrile and the photon $h\nu_2$. An appealing aspect of the single-molecule single-photon double-excitation scheme is the potential ability to resolve in time the consecutive excitation processes. In
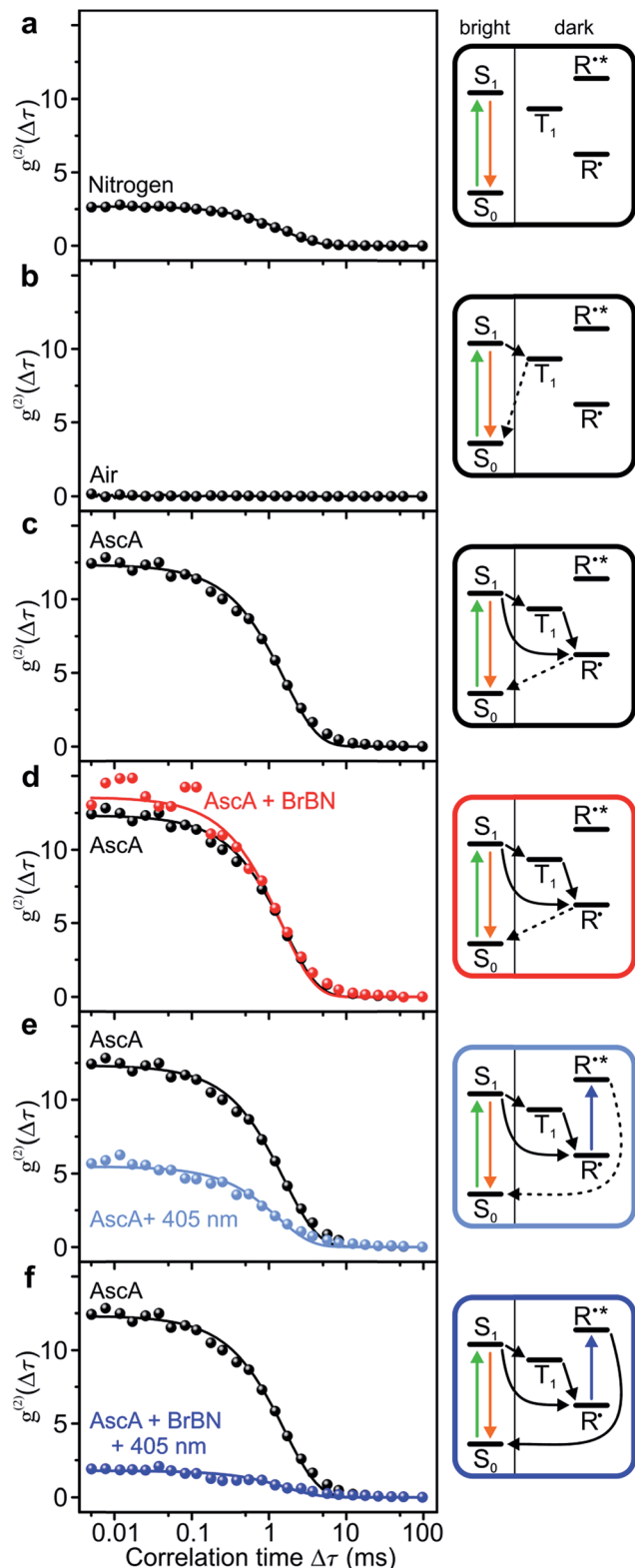
Fig. 3 Control of fluorescence intensity correlations of single Rh6G molecules through the reaction conditions. The plots show median values of the correlations at each time $\Delta\tau$ for one hundred single molecules each, with single-exponential fits. The level schemes responsible for each correlation signal are indicated on the right. (a) Rh6G in N_2-saturated solution. (b) Rh6G in air-saturated solution. (c) Rh6G in N_2-saturated solution with the reducing agent ascorbic acid (AscA) added. (d) As in panel c but with the substrate 2-

a double-pulse experiment, for example, it should be possible to measure directly the lifetime of the photoexcited radical by varying the duration of the $h\nu_2$ pulse. In addition, tuning the energy $h\nu_2$ in a "photocatalytic action" experiment may even allow time-resolved probing of conformational relaxation dynamics of the catalytically active dye which would offer crucial insight for quantum-chemical modelling of the molecular dynamics of the catalyst–substrate interaction. In this context, we derive two conclusions from the observations. First, the photocatalytic reaction is not fundamentally diffusion limited. Since the lifetime of the photoexcited radical $R^{\bullet*}$ is expected to be extremely short,[48] the conPET process can only occur if the substrate molecule is preassociated with the dye catalyst. Second, to prevent product inhibition of the catalyst and enable continued observation of the photocatalytic cycle in fluorescence, the reacted species must dissociate from the catalyst to allow the reaction to begin anew. We propose that the radical exerts an attractive force on the substrate, promoting preassociation, and speculate that such an effect may be more common to photocatalytic processes than previously thought. While we cannot conclusively prove that preaggregation does not occur in the dye ground state, we reiterate the observed reduction in turnover number upon dehalogenation of the substrate, implying that interaction with either form of the dye must be weakened. We note that the substrate is an aromatic system with two electron-withdrawing substituents. The interaction of such an electron-poor aromatic should be stronger with the neutral dye radical than with the cationic dye ground state. As discussed above, depending on the protonation balance, the rhodamine ground state may actually be neutral. In this case, the interaction of the dye with the electron-poor substrate would also be stronger in the anionic radical state than in the neutral ground state. Without precise determination of the different contributions from van der Waals interactions, pi-stacking and electrostatics, such arguments, however, remain qualitative. To further explore the microscopic origins of this phenomenon will necessitate the development of time-dependent density functional theory (TD-DFT) techniques which can take into account the strong polarization effects of the surrounding medium.[51] This can be achieved by implementing new theoretical methods to account for the complex excited-state geometry optimization arising from the non-adiabatic molecular dynamics. To arrive at such a microscopic theory of organic photocatalysis it is imperative to have access to truly microscopic experimental data, which only become available on the single-molecule level. An open question is whether the trapping agent N-methylpyrrole used in the ensemble experiments also sticks to the photocatalyst. This could conceivably be expected since dispersive interactions should be of a comparable nature to those of the substrate, but such an association could in turn block the photocatalyst. Given near-unity conversion yields found in the ensemble, such blocking is apparently unlikely.

bromobenzonitrile (BrBN) added. (e) As in panel c but with $h\nu_2$ added. (f) As in panel e but with 2-bromobenzonitrile added. Only in this last case is the dark state of the fluorophore removed by the closed conPET cycle and the correlation curve appears flat.

Fig. 4 Control measurements of the fluorescence intensity correlation with non-reacting substrate molecules for the four conditions in Fig. 3c–f. (a) Non-halogenated substrate benzonitrile (BN). (b) Substrate 4-chloroanisole (ClAn). The reduction potential of this compound is too high for the photoexcited Rh6G radical.

Our crucial conclusion is that in mechanisms which involve preassociation of substrate and photocatalyst, diffusion no longer appears to be the limiting factor so that long excited-state lifetimes are not necessary to ensure effective photocatalytic transformation. This is an important point since most photoredox catalytic cycles involve long-lived triplet states. Triplets, however, limit the overall catalytic potential since electronic energy is inherently lost to the quantum–mechanical exchange interaction by satisfying Pauli's exclusion principle. Our work therefore encourages a renewed search for materials supporting singlet-based photoredox cycles. The dehalogenation reaction demonstrated here on the single-molecule single-photon level constitutes a precursor to more complex photocatalytic mechanisms. We expect the cycle to work equally well in forming carbon–carbon bonds, opening up the possibility of multicolour directed synthesis[13] on the single-molecule level.

Conflicts of interest

There are no conflicts to declare.

Acknowledgements

References

1 N. A. Romero and D. A. Nicewicz, *Chem. Rev.*, 2016, **116**, 10075–10166.
2 C. K. Prier, D. A. Rankic and D. W. C. MacMillan, *Chem. Rev.*, 2013, **113**, 5322–5363.
3 D. M. Arias-Rotondo and J. K. McCusker, *Chem. Soc. Rev.*, 2016, **45**, 5803–5820.
4 D. M. Schultz and T. P. Yoon, *Science*, 2014, **343**, 985–988.
5 J. Xuan and W. J. Xiao, *Angew. Chem., Int. Ed.*, 2012, **51**, 6828–6838.
6 D. A. Nicewicz and D. W. C. MacMillan, *Science*, 2008, **322**, 77–80.
7 H. Kim and C. Lee, *Angew. Chem., Int. Ed.*, 2012, **51**, 12303–12306.
8 M. H. Shaw, J. Twilton and D. W. C. MacMillan, *J. Org. Chem.*, 2016, **81**, 6898–6926.
9 Y. Du, R. M. Pearson, C. H. Lim, S. M. Sartor, M. D. Ryan, H. S. Yang, N. H. Damrauer and G. M. Miyake, *Chem.–Eur. J.*, 2017, **23**, 10962–10968.
10 I. Ghosh, L. Marzo, A. Das, R. Shaikh and B. König, *Acc. Chem. Res.*, 2016, **49**, 1566–1577.
11 D. Ravelli, M. Fagnoni and A. Albini, Photoorganocatalysis. What for?, *Chem. Soc. Rev.*, 2013, **42**, 97–113.
12 I. Ghosh, T. Ghosh, J. I. Bardagi and B. König, *Science*, 2014, **346**, 725–728.
13 I. Ghosh and B. König, *Angew. Chem., Int. Ed.*, 2016, **55**, 7676–7679.
14 E. Yoshioka, S. Kohtani, T. Jichu, T. Fukazawa, T. Nagai, A. Kawashima, Y. Takemoto and H. Miyabe, *J. Org. Chem.*, 2016, **81**, 7217–7229.
15 E. Yoshiokaa, S. Kohtani, T. Jichu, T. Fukazawa, T. Nagai, Y. Takemoto and H. Miyabe, *Synlett*, 2015, **26**, 265–270.
16 M. Orrit, *Angew. Chem., Int. Ed.*, 2015, **54**, 8004–8005.
17 M. Marchini, G. Bergamini, P. G. Cozzi, P. Ceroni and V. Balzani, *Angew. Chem., Int. Ed.*, 2017, **56**, 12820–12821.
18 J. W. Tucker and C. R. J. Stephenson, *J. Org. Chem.*, 2012, **77**, 1617–1622.
19 I. Ghosh, J. I. Bardagi and B. König, *Angew. Chem., Int. Ed.*, 2017, **56**, 12822–12824.
20 M. B. J. Roeffaers, B. F. Sels, H. Uji-i, F. C. De Schryver, P. A. Jacobs, D. E. De Vos and J. Hofkens, *Nature*, 2006, **439**, 572–575.
21 M. B. J. Roeffaers, G. De Cremer, J. Libeert, R. Ameloot, P. Dedecker, A. J. Bons, M. Buckins, J. A. Martens, B. F. Sels, D. E. De Vos and J. Hofkens, *Angew. Chem., Int. Ed.*, 2009, **48**, 9285–9289.
22 F. C. Hendriks, S. Mohammadian, Z. Ristanovic, S. Kalirai, F. Meirer, E. T. C. Vogt, P. C. A. Bruijnincx, H. C. Gerritsen and B. M. Weckhuysen, *Angew. Chem., Int. Ed.*, 2018, **57**, 257–261.
23 K. Naito, T. Tachikawa, M. Fujitsuka and T. Majima, *J. Phys. Chem. B*, 2005, **109**, 23138–23140.
24 T. Tachikawa and T. Majima, *Chem. Soc. Rev.*, 2010, **39**, 4802–4819.
25 N. Wang, T. Tachikawa and T. Majima, *Chem. Sci.*, 2011, **2**, 891–900.

26 B. de Nijs, F. Benz, S. J. Barrow, D. O. Sigle, R. Chikkaraddy, A. Palma, C. Carnegie, M. Kamp, R. Sundararaman, P. Narang, O. A. Scherman and J. J. Baumberg, *Nat. Commun.*, 2017, **8**, 994.

27 B. Hulsken, R. Van Hameren, J. W. Gerritsen, T. Khoury, P. Thordarson, M. J. Crossley, A. E. Rowan, R. J. M. Nolte, J. Elemans and S. Speller, *Nat. Nanotechnol.*, 2007, **2**, 285–289.

28 T. Adachi, J. Vogelsang and J. M. Lupton, *J. Phys. Chem. Lett.*, 2014, **5**, 573–577.

29 P. Chen, X. C. Zhou, H. Shen, N. M. Andoy, E. Choudhary, K. S. Han, G. K. Liu and W. L. Meng, *Chem. Soc. Rev.*, 2010, **39**, 4560–4570.

30 T. Christ, F. Kulzer, P. Bordat and T. Basché, *Angew. Chem., Int. Ed.*, 2001, **40**, 4192–4195.

31 M. B. J. Roeffaers, G. De Cremer, H. Uji-i, B. Muls, B. F. Sels, P. A. Jacobs, F. C. De Schryver, D. E. De Vos and J. Hofkens, *Proc. Natl. Acad. Sci. U. S. A.*, 2007, **104**, 12603–12609.

32 K. P. F. Janssen, G. De Cremer, R. K. Neely, A. V. Kubarev, J. Van Loon, J. A. Martens, D. E. De Vos, M. B. J. Roeffaers and J. Hofkens, *Chem. Soc. Rev.*, 2014, **43**, 990–1006.

33 H. Yang, G. B. Luo, P. Karnchanaphanurach, T. M. Louie, I. Rech, S. Cova, L. Y. Xun and X. S. Xie, *Science*, 2003, **302**, 262–266.

34 T. J. Ha, A. Y. Ting, J. Liang, W. B. Caldwell, A. A. Deniz, D. S. Chemla, P. G. Schultz and S. Weiss, *Proc. Natl. Acad. Sci. U. S. A.*, 1999, **96**, 893–898.

35 R. D. Smiley and G. G. Hammes, *Chem. Rev.*, 2006, **106**, 3080–3094.

36 H. P. Lu and X. S. Xie, *J. Phys. Chem. B*, 1997, **101**, 2753–2757.

37 W. Ho, *J. Chem. Phys.*, 2002, **117**, 11033–11061.

38 L. Lafferentz, F. Ample, H. Yu, S. Hecht, C. Joachim and L. Grill, *Science*, 2009, **323**, 1193–1197.

39 S. W. Hla, L. Bartels, G. Meyer and K. H. Rieder, *Phys. Rev. Lett.*, 2000, **85**, 2777–2780.

40 D. G. de Oteyza, P. Gorman, Y. C. Chen, S. Wickenburg, A. Riss, D. J. Mowbray, G. Etkin, Z. Pedramrazi, H. Z. Tsai, A. Rubio, M. F. Crommie and F. R. Fischer, *Science*, 2013, **340**, 1434–1437.

41 I. Swart, L. Gross and P. Liljeroth, *Chem. Commun.*, 2011, **47**, 9011–9023.

42 T. Basché, W. E. Moerner, M. Orrit and H. Talon, *Phys. Rev. Lett.*, 1992, **69**, 1516–1519.

43 T. Basché, S. Kummer and C. Bräuchle, *Nature*, 1995, **373**, 132–134.

44 M. Vester, T. Staut, J. Enderlein and G. Jung, *J. Phys. Chem. Lett.*, 2015, **6**, 1149–1154.

45 T. Slanina and T. Oberschmid, *ChemCatChem*, 2018, **10**, 4182–4190.

46 M. Neumeier, D. Sampedro, M. Majek, V. A. de la Peña O'Shea, A. Jacobi von Wangelin and R. Pérez-Ruiz, *Chem.–Eur. J.*, 2018, **24**, 105–108.

47 S. Doose, H. Neuweiler and M. Sauer, *ChemPhysChem*, 2009, **10**, 1389–1398.

48 D. Gosztola, M. P. Niemczyk, W. Svec, A. S. Lukas and M. R. Wasielewski, *J. Phys. Chem. A*, 2000, **104**, 6545–6551.

49 M. Heilemann, R. Kasper, P. Tinnefeld and M. Sauer, *J. Am. Chem. Soc.*, 2006, **128**, 16864–16875.

50 W. T. Yip, D. H. Hu, J. Yu, D. A. Vanden Bout and P. F. Barbara, *J. Phys. Chem. A*, 1998, **102**, 7564–7575.

51 Z. Zheng, D. A. Egger, J.-L. Brédas, L. Kronik and V. Coropceanu, *J. Phys. Chem. Lett.*, 2017, **8**, 3277–3282.

52 J. Vogelsang, R. Kasper, C. Steinhauer, B. Person, M. Heilemann, M. Sauer and P. Tinnefeld, *Angew. Chem., Int. Ed.*, 2008, **47**, 5465–5469.

53 S. van de Linde, I. Krstić, T. Prisner, S. Doose, M. Heilemann and M. Sauer, *Photochem. Photobiol. Sci.*, 2011, **10**, 499–506.